

[DRAFT] Array Optimization of Fixed Oscillating Water Columns for Active Device Control

Chris Sharp*[†] Bryony DuPont*, Bret Bosma*, Pedro Lomonaco* and Belinda Batten*

*Northwest National Marine Renewable Energy Center

*Oregon State University, Corvallis, OR, USA

[†]sharpc@oregonstate.edu

Abstract—Realizing the vast amount of energy available in ocean waves, an industry has emerged that is progressing towards the deployment of grid-connected wave energy devices. Likely to be deployed in grouped scenarios, a challenge to wave energy is maximizing the energy production of such arrays. Active device control and array design optimization are two methods of achieving increased power. Our work is in the development of a metaheuristic system array optimization method specifically for the optimization of wave energy converter arrays. As a preliminary step, we are testing our array optimization algorithm with five scaled oscillating water columns. These devices are being built and will be used to evaluate the coordination of device control in an array setting. Finding that configurations differ in shape and power production based on wave condition and devices damping, we present our novel method for determining optimal arrangements of an array through the use of a problem specific genetic algorithm and device BEM model.

Index Terms—Wave Energy, OWC, Array, Optimization, Design

I. INTRODUCTION

As the wave energy industry advances towards the deployment of offshore, grid-connected devices, it is important to prepare for how these wave energy converters (WECs) will ultimately be implemented on a larger scale. In light of the progression of the wind and solar industries, the wave energy industry will likely follow a similar trajectory and ultimately deploy WECs in array scenarios utilizing advanced device control techniques.

Regarding WEC array design, most research has focused on empirical layouts – assumed layouts given a designer’s best understanding of how devices behave and interact in a wave field. However, the complexity of the ocean space excludes these solutions from being readily used by industry. As such, research has shifted towards leveraging automated optimization methods to generate potential layout designs by better exploring and exploiting the search space.

In addition to the likely implementation of WECs in arrays, it is expected that for WECs to be economically feasible, active control scenarios must be implemented to fully maximize power production. Consequently, it is necessary that we

consider optimal array layouts in conjunction with active device control. As a part of the Advanced Laboratory and Field Arrays (ALFA) project (a US Department of Energy funded project), we have been working on determining optimal device arrangement of an oscillating water column (OWC) array. These optimized layouts will be used as an input for implementing active control and ultimately we will tank test an array(s) of actively controlled devices.

In this paper we discuss an overview of our task within the project; prior optimization approaches to WEC array design; the tank-validated, boundary element method (BEM) model of our OWC; the optimal layouts generated by our problem specific genetic algorithm (GA); and our initial analysis of the power output sensitivity due to damping control and array design. The achieved layouts will indicate the influence of sea state on device configuration and will show the need for active device control.

II. PROJECT OVERVIEW

Of the ALFA project’s many directives, we are specifically investigating the enhancement of WEC array performance. The goals of our task include generating optimal configurations of a WEC array, developing control strategies for the devices within these arrays, and validating the use of these control strategies on an optimized array through tank testing.

To achieve the first of these goals, we model our selected device using a boundary element method, validate this model, and then determine an optimal arrangement of five devices – with minimization of negative power as the objective function. Because the devices being constructed are only intended for tank testing and the number of devices is fixed at five, cost has been excluded from the objective function. Active control scenarios will later be tested on this arrangement by others on the project and we will validate the array optimization and control results against tank test data later this year. More information can be found on the modeling and physical testing of our chosen device in [1].

An objective of our work is to better understand the integration of active control with array optimization. With the stochasticity of sea conditions, actively controlling devices within an array is believed to likely have greater influence on increasing power production than what can be achieved through array optimization of non-controlled devices [2], [3]. With the effectiveness of device control [4], future array power models should incorporate such active control. Unfortunately a model does not currently exist that includes both between-device wave interaction and active control. This work will serve as a basis for the future inclusion of active control into an optimization scheme.

III. ARRAY OPTIMIZATION

A. Previous Work

Given the current implementation barriers for deploying even a single WEC device, attention to WEC array design has only recently begun gaining momentum. Based on studies of the wave fields created by devices in grouped scenarios, the possibility of attaining increased power due to positive device-device wave interaction has been theorized [5]–[8]. Referred to as the interaction factor, q , this interaction is defined as

$$q = \frac{P_{array}}{N * P_i} \quad (1)$$

where P_i is the power generated by a single device in isolation, N is the number of devices in an array, and P_{array} is the power generated by that array [8]. Values of q less than one indicate a loss in power due to negative interactions between devices and values greater than one indicate a gain in power. Research thus far in array design has been driven by the desire to maximize the interaction factor [9]–[12].

Array design has primarily consisted of creating and comparing prescribed layouts such as lines (both parallel and orthogonal to the oncoming wave), triangles, squares, and various grid designs [10]–[15]. Furthering this research, automated layout optimization methods are being utilized and developed.

Using a point approximation to determine WEC array power production, Fitzgerald and Thomas implement a sequential quadratic algorithm based on a selected starting point [16]. Considering two variations of a GA and a greedy algorithm, Mao determines that the GA is the better approach because similarity lacks between optimal layouts of varying device numbers [17]. Snyder and Moarefdoost present two optimization methods, a max-min model and a maximization expected value model, to account for variability in incident wave direction [18]. They determine that an increase in uncertainty yields a decrease in optimal spacing between two devices. Moarefdoost et al. later presents a heuristic algorithm that exploits solutions believed to be near optimal [19]. Mao, Snyder and Moarefdoost, and Moarefdoost et al. all use the

point approximation method and consider only regular waves.

Child and Venugopal investigate the optimization of WEC arrays using MATLAB’s GA toolbox and introduce the Parabolic Intersection (PI) method [20]. The PI method is based on the assumption that a WEC’s wake is in the shape of parabola and that downwave devices should be placed at the intersections of upwave wakes to generate greater power. They determine that the PI method obtains results similar to those of the GA, but that the GA outperforms the PI method overall. The PI method is noted to be computationally more efficient however.

More recently, a device-specific machine learning approach has been applied to the WEC array optimization problem by Sarkar et al. [21]. Evaluating a bottom mounted flap type WEC, it is determined that, for submerged, surge-type devices, clustering should be avoided. Wu et al. also examines a submerged type device and implements two evolutionary type algorithms, a (1+1)-EA algorithm and a Covariance Matrix Adaptation based Evolutionary Strategy (CMA-ES) [22]. Optimizing an array of mid-water column, floating spheres, the methods do not perform well independently. However, when the (1+1)-EA is used to get close to converging on a solution, the CMA-ES is able to fine-tune that solution.

McGuinness and Thomas have created a purely analytical method of optimizing the spacing between WECs that are placed in a row [23]. Observing that in certain scenarios devices tend to cluster, they postulate that these devices could be replaced with a larger device to minimize physical device interaction, but still achieve increased power production. The optimal spacings also differ depending on the direction of the incident wave.

B. Current Optimization Scheme

Noting the need to include more array configuration influencers, we have developed a genetic algorithm (GA) specific to the problem of WEC array design that furthers the work of existing research.

The complexity of the array optimization problem is not limited to determining the power produced by an array, but should also include alternative factors which might alter an array’s design. Some of these, such as cost and active device control, will likely have significant influence on a layout’s configuration. Our GA currently allows for the inclusion of array cost in addition to power [24], [25]; however, since the number of devices being tested is fixed and the devices are solely intended for tank testing, we have simplified the objective function to only consider generated power. This will aid in ultimately including device control in the objective function through variable device damping.

IV. METHODOLOGY

To achieve optimal layouts, we first model a single device using the boundary element software, WAMIT [26]. This informs how a device behaves in a given wave field for a range of wave directions – specifically, we obtain the OWC’s added mass, hydrodynamic damping, hydrodynamic restoring force, and excitation force. The developed GA will then create generations of potential layouts based on the process of *survival of the fittest* in combination with how chromosomes are shared between generations.

Within this process there are several sets of code that must be linked together. The inputs and outputs of each set of code and the appropriate linkages are described here.

- **WAMIT**: A boundary element software used to determine how waves interact with offshore devices. For our project, the outputs required of WAMIT are the added mass, hydrodynamic damping, hydrodynamic restoring force, and excitation force of a single OWC (for a single water depth and a range of wave periods/directions).
- **mwave**: A MATLAB computational package developed by Cameron McNatt out of the University of Edinburgh for evaluating WEC(s) and ocean waves. We are using *mwave* both as a pre and post-processor for WAMIT and for determining an array’s power output such that device-to-device wave interactions are included.
- **real-coded GA**: The algorithm we are developing for the purpose of determining optimal layout designs such that power and cost can be included. This algorithm is being written in MATLAB specifically to interface with the other programs.

With a fixed number of devices intended for tank testing, our optimization centers around the maximization of power. As such the objective function we are seeking to minimize is

$$ObjFun = -P_{20} \quad (2)$$

where P_{20} is the power generated by an array over a 20 year lifespan. The process components are visually shown in Fig. 1 and each component will be discussed in the following sections.

A. OWC Modeling

We have produced layout configurations of scaled, representative heaving point absorbers in both the discrete and continuous spaces [24], [25]. In continuation, we are now optimizing the arrangement of fixed oscillating water columns (OWCs). We chose oscillating water columns partly because the technology has been in existence for some time, but primarily because several devices could be inexpensively built and tank tested.

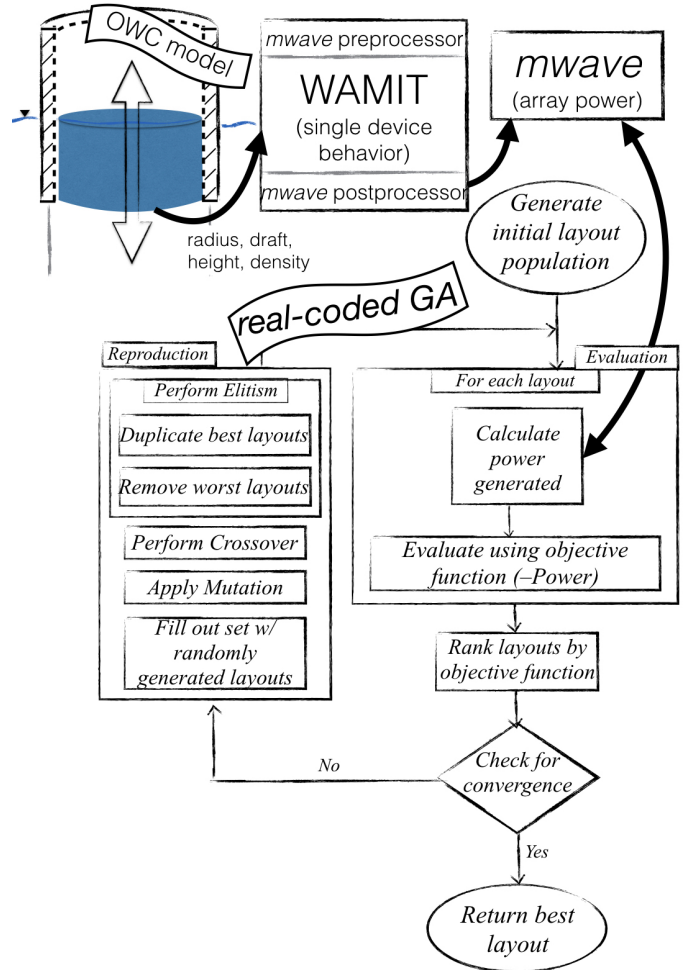


Fig. 1. OPTIMIZATION PROCESS OVERVIEW

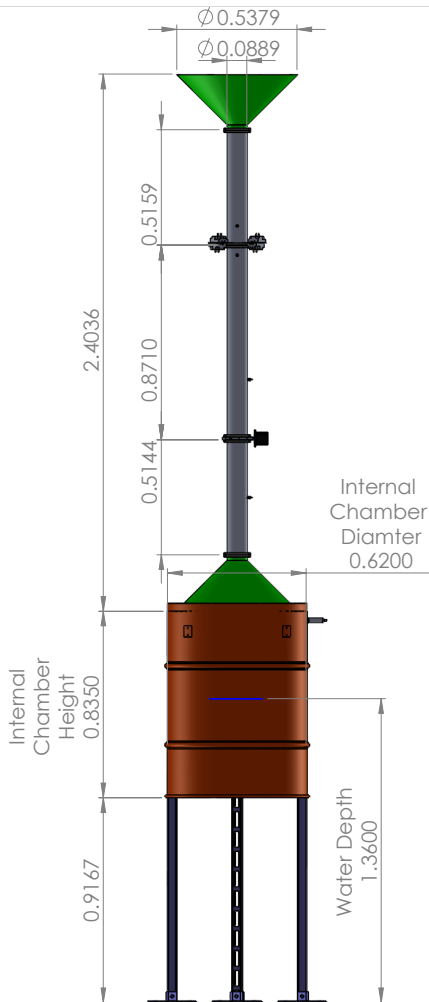
For this project, five physical devices are being constructed. Figure 2(a) is an image of the first of these OWCs and Fig. 2(b) shows its dimensions. The remaining four devices are built in the same manner.

An OWC operates by having a hollow cylinder extend both above and below the water surface. As the water rises and falls, air is forced in and out of the hollow interior through the cylinder’s narrower, above-water component. If this device were to be used as an energy producer, the flow of air would likely turn a bidirectional turbine which would then generate electricity. For our work, a butterfly valve is used in place of a turbine due to it’s measurability and controllability. This valve can rotate between 0° and 90° where 0° indicates the valve completely closed and 90° indicates a completely open valve. Specific details on this can be found in the corresponding study by Bosma et al. [1].

To evaluate potential layouts of OWCs in search of an optimal solution, we need the added mass, hydrodynamic damping, hydrodynamic restoring force, and excitation force of a single device at a fixed water depth for a range of wave



(a) PHOTO OF PHYSICAL DEVICES BEING BUILT



(b) SCHEMATIC OF PHYSICAL DEVICE(S)

Fig. 2. PHYSICAL DEVICE

periods and directions. To obtain these, we model the OWC shown in Fig. 2 within WAMIT. Developed by Evans [27] and described in [28]–[31], the OWC can be modeled using a piston approach. This method treats the mass of water moving inside the cylinder as a heaving point absorber. Since the OWC is to be secured to the tank floor, the model needs to only be a single body.

The water depth and desired wave periods are used as inputs into WAMIT along with the radius, draft, height and density of the representative point absorber. In our case, the radius is 0.31 m, the draft (distance below the still water surface) is 0.44 m, the height (total height of the piston) is also 0.44 m, and the density is 1000 kg/m^3 . *Mwave* creates the necessary input files for WAMIT as a preprocessor and, once WAMIT has completed running, processes the output data to formulate an object containing the information needed to analytically determine an array's power output. The theory behind *mwave* is described in [15], [32].

WAMIT details how a device behaves for a range of wave periods and directions at a single water depth. It only needs to be run once at the beginning of the optimization process – unless a physical device parameter is changed or a different sea conditions is desired (i.e. differing draft or water depth). Showing the RAO output from WAMIT and the experimentally determined RAO, Fig. 3 indicates the viability of our developed BEM model.

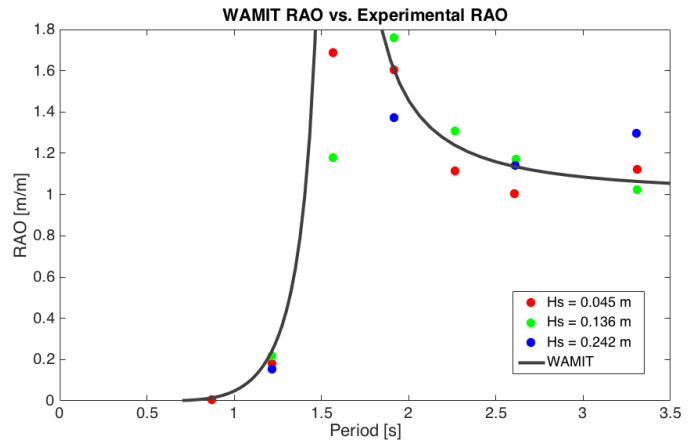


Fig. 3. RAO COMPARISON BETWEEN WAMIT RESULTS AND TANK DATA

The output of WAMIT is needed by the power calculation within *mwave*. *Mwave*, and consequently the outputted MATLAB object, are called for every uniquely created layout within the *real-coded GA*

B. Array Optimization

With the information derived from WAMIT, we begin the *real-coded GA* process. Even without guaranteeing global optimality, our GA method was, and is continually being, developed because of its ability to handle the stochasticity

surrounding WEC array optimization. GAs are based on the biological process of children being a combination of their parent’s chromosomes along with the potential for mutation throughout the creation of a new generation. A population based optimization approach, sets of potential solutions are created, evaluated, sorted, and used to create the next set of potential solutions. This process occurs through several specific steps within our *real-coded GA* – elitism, crossover, mutation, and random generation.

Besides the initial generation of potential solutions, which is made entirely by random WEC placement, each generation of children begins with elitism. Before populating the next generation, the previous is evaluated and sorted such that the best solutions (those with the smallest objective function found from Eq. 2) are at the top and the worst solutions are at the bottom. Elitism then occurs by cloning the best solutions from the parent set to the child set. Exact copying of the best solution(s) ensures that the overall-best solution is not inadvertently lost between generations. As a secondary portion to elitism, slightly mutated versions of the cloned solutions are also added to the child population. These are created to better exploit the best solution(s) in the hope of finding an even better solution.

The next portion of child solutions are created through crossover. Crossover occurs by taking pairs from an upper percentage of the parent generation and combining them to create two children that are each a semblance of both parents. Pairings are selected by rank roulette. After a pair of children is created they are each subject to the possibility of mutation. Mutation is when a device(s) is randomly selected within a layout and moved to a new location. Finally, to keep exploring the solution space and to ensure consistency in population size between generations, layouts with randomly placed WECs are added into the new population.

Our algorithm best searches the solution space with implemented stochasticity. Therefore, the rates of elitism and crossover are both tunable and should be set so that there is space to fill in the new generation with random solutions. The real-coded GA flowchart in Fig. 1 shows the progression of steps. Table I contains the tunable parameters within the GA and the assigned values for the work presented in this paper. Detailed specifics on the workings of our *real-coded GA* can be found in [25].

Since every generation of children becomes a parent generation and continues the reproduction cycle, a convergence criteria is defined to conclude the algorithm. As indicated in Table I, 100 generations must occur without finding a new best overall solution before the GA will stop and return the best layout. Because the search space is infinite and stochastic, the GA repeats several times for each scenario and we are presenting the overall best of the resultant layouts.

TABLE I
TUNABLE GA PARAMETERS

# Of Parents	100
Elitism Rate	2%
Crossover & Mutation Rate	74%
Crossover Probability	100%
Mutation Probability	35%
Max # of WECs to Mutate	2
Convergence Requirement (generations without improvement)	100

For this work, we run a total of 18 different wave scenarios. A water depth of 1.36 meters and wave height of 0.136 meters is consistent across all cases while the wave period, valve angle, and wave type (regular or irregular) are varied. For all cases the damping values come from tank testing a single device in regular waves with the shown significant wave height and periods. The devices are required to be a minimum of 3 times their diameter away from neighboring devices (this distance is measured from center to center) to mimic real sea constraints. Table II shows the considered scenarios.

We are specifically looking to observe the potential impact of three variables – wave period, wave type (regular versus irregular), and damping (valve angle).

V. RESULTS

A. Fixed Valve Angle - 44°

We first generate optimal layouts while considering a constant valve angle of 44°. Six cases of regular waves and four cases of irregular waves are run. With the valve angle constant, the damping fluctuates between each run as a result of a changing wave period. For all cases, waves are traveling from left to right. The physical space is tunable within the *real-coded GA* so each scenario is run through several different sized spaces to ensure that no physical space constraint is inadvertently enacted. The dimensions of each figure indicate the dimensions at which the best layout is found.

1) *REGULAR Waves*: The wave periods for the regular wave cases range from 1.22 seconds to 3.31 seconds with a consistent wave height of 0.136 meters. Each scenario is run multiple times and the layouts found yielding the best interaction factors are shown in Fig. 4.

Observing the layouts obtained with regular waves, we note that in all scenarios the GA is able to generate a configuration with an interaction factor greater than one. These interaction factors greatly depend on the incident wave period and behave much better with the shorter wave periods tested. For a period of 1.22 seconds a layout is found that yields an interaction

TABLE II
WAVE SCENARIOS

Regular Wave Cases			
Valve Angle	Wave Height [m]	Period [s]	Damping [N/(m/s)]
80°	0.136	1.22	107.1
44°			363.9
0°			3316.2
44°	0.136	1.57	640.6
44°		1.91	774.7
44°		2.26	891.0
44°		2.61	892.4
80°	0.136	3.31	293.0
44°			775.2
0°			10032.5
Irregular Wave Cases			
Valve Angle	Significant Wave Height [m]	Peak Period [s]	Damping [N/(m/s)]
80°	0.136	1.22	107.1
44°			363.9
0°			3316.2
44°	0.136	1.91	774.7
44°		2.61	892.4
80°	0.136	3.31	293.0
44°			775.2
0°			10032.5

factor of 2.579 (Fig. 4(a)). For the longest tested period, 3.31 seconds, an interaction factor of 1.0257 (Fig. 4(f)) is obtained. This behavior is expected since a shorter period means that the device will undergo more oscillations in a set amount of time when compared to longer periods. The results from the shorter periods (Figs. 4(a) & 4(b)) indicate devices taking advantage of individual neighbor's diffracted waves. The increased periods (Figs. 4(c), 4(d) & 4(e)) show devices acting in groups that place themselves in semi-parallel lines perpendicular to the incident waves. Figure 4(f) shows devices pairing up and benefiting from another paired device's diffracted waves.

2) *IRREGULAR Waves*: We also obtained layouts for irregular wave conditions with a valve angle of 44°. The waves are generated based on a Bretschneider spectrum and have a significant wave height of 0.136 meters. We considered two different wave periods and the results are shown in Fig. 5.

As with the layouts obtained using regular waves, the layouts obtained with the 44° valve angle in irregular waves obtain interaction factors consistently greater than one and follow

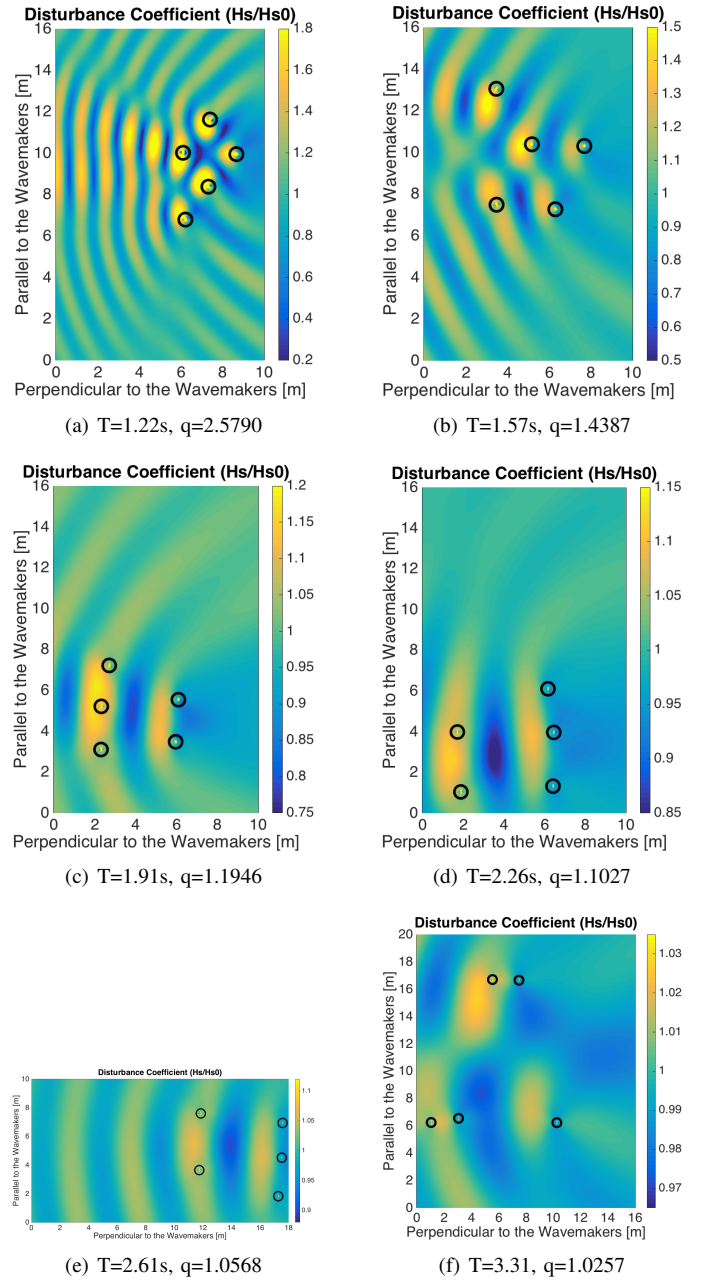


Fig. 4. OPTIMAL LAYOUTS WITH REGULAR WAVES, A VALVE ANGLE OF 44° AND H = 0.136m

a similar trend to the regular waves. The shorter period in Fig. 5(a) shows devices acting individually and the rest show devices acting in groups. The longer waver periods (shown in Figs. 5(c) & 5(d)) indicate the devices grouping and then creating space between the groups. This is likely in order to allow the diffracted waves of the first group to begin filling in before reaching the second group. The increase in interaction factor from these scenarios is likely due to the subgroups of devices more so than the entire group of devices.

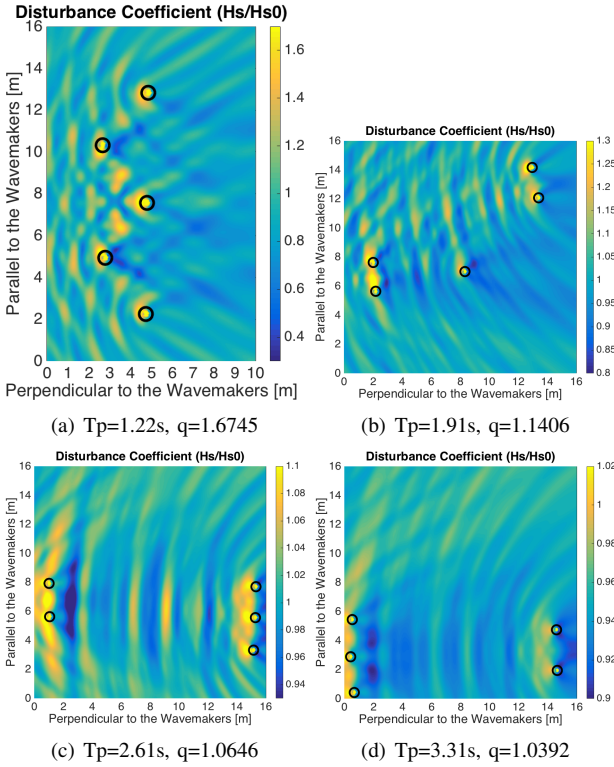


Fig. 5. OPTIMAL LAYOUTS WITH IRREGULAR WAVES, A VALVE ANGLE OF 44° , AND $H_{mo} = 0.136\text{m}$

B. Varied Valve Angles

To further understand how device control might affect the power production we also look at different simulated valve angles (experienced through changing the damping value) in both regular and irregular wave conditions. The damping values come from regular wave tests of an OWC in the wave tank and are listed in Table II. They range from 107.1 N/(m/s) at the shortest wave period and 80° to 100032.5 N/(m/s) at the longest wave period and 0° . We select the damping values from the extreme valve positions to gain understanding into the effect on power over the full range of valve angles. We can compare these results with the damping values from the valve angle of 44° that is between these extremes. For the irregular wave scenarios, a Bretschneider spectrum is chosen for consistency with our previous work [24], [25].

1) *REGULAR Waves*: Having already shown the results found for a 44° valve angle, Fig. 6 shows the best layouts obtained when optimizing the array with a valve angle almost completely open at 80° . Based on the data from a tank test of a single OWC, a fixed valve angle will cause damping changes dependent on the incident wave. The 80° scenarios simulate devices allowing close to the maximum amount of air flow in and out of the interior chamber of the OWC.

The next valve angle we consider with regular waves is 0° — to mimic when the valve is completely shut. Though an oscillating water column would be unable to generate

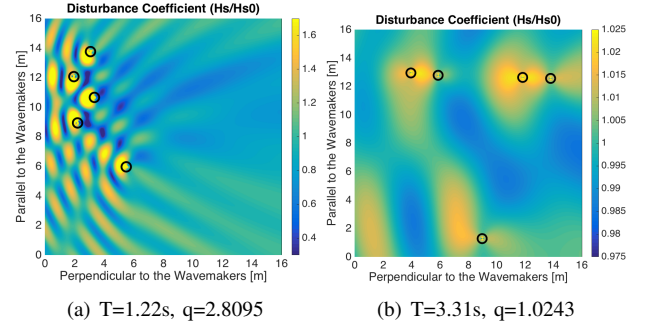


Fig. 6. OPTIMAL LAYOUTS WITH REGULAR WAVES, A VALVE ANGLE OF 80° AND $H = 0.136\text{m}$

power without air flow, we use this scenario to compare what interaction could be obtained with the maximum damping created by this valve position. The resulting layouts and corresponding interaction factors are displayed in Fig. 7.

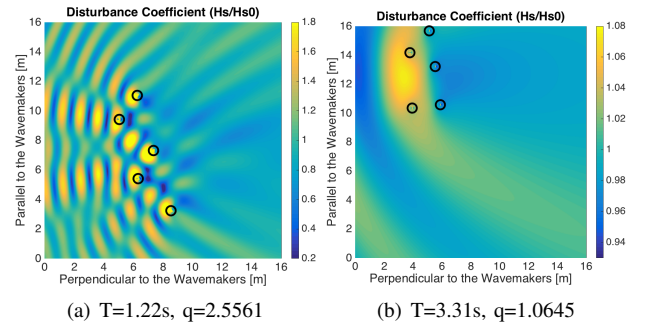


Fig. 7. OPTIMAL LAYOUTS WITH REGULAR WAVES, A VALVE ANGLE OF 0° , AND $H = 0.136\text{m}$

The 80° scenarios follow a trend similar to the previous results seen in the layouts generated for the shorter and longer wave periods. Shorter periods yield individual behavior and longer periods yield grouping behavior. However, the result in Fig. 9(b) for the 0° scenario indicates devices acting individually even with the longer period.

2) *IRREGULAR Waves*: We now look at the behavior observed for different valve positions under irregular wave conditions. The same valve positions and wave conditions are evaluated as in the regular wave scenarios. Based on the results of the fixed valve angle we expect to see results that have similar tendencies as regular waves. With irregular waves and a valve angle of 80° , The best layouts found when the valve is almost completely open are shown in Fig. 8. The resulting layouts again show devices taking individual advantage of neighboring devices for the shorter period and separating into two distinct groups for the longer period.

The last valve angle we consider with irregular waves is 0° . The layouts determined are shown in Fig. 9 and yield similar layouts to the regular waves with a valve angle of 0° . Both periods seem to indicate devices acting individually; however,

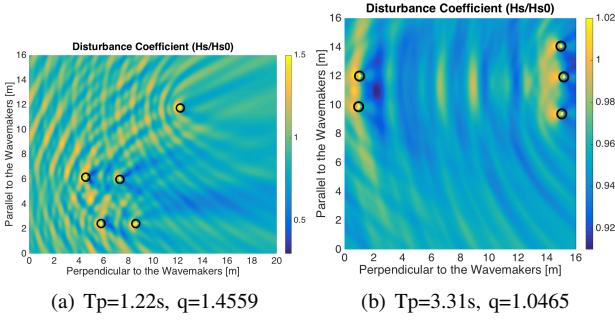


Fig. 8. OPTIMAL LAYOUTS WITH IRREGULAR WAVES, A VALVE ANGLE OF 80° AND $H_{m0} = 0.136\text{m}$

as Table III shows the shorter period provides a much higher power improvement. This trend, beyond the observed trends in configuration shape, will be discussed further in the next section.

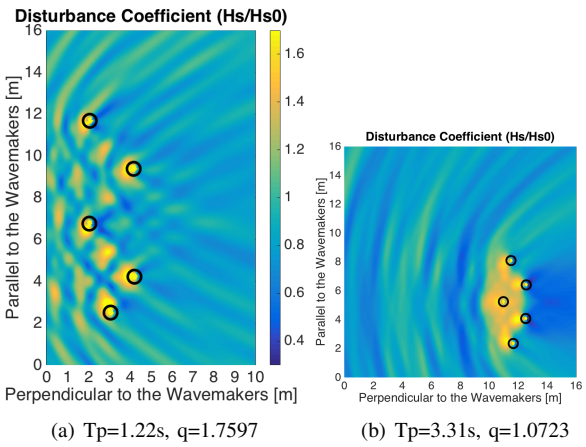


Fig. 9. OPTIMAL LAYOUTS WITH IRREGULAR WAVES, A VALVE ANGLE OF 0° AND $H_{m0} = 0.136\text{m}$

VI. DISCUSSION

Running a total of 18 different scenarios, we are able to preliminarily understand the considerations of WEC array optimization in conjunction with active device control. The results from the runs are compiled in Table III. The number of generations in the last column refers to how many cycles the *real-coded GA* went through before converging. Based on our convergence requirement the optimal layout would have been found 100 generations prior to the value shown.

Examining Table III we note certain behaviors dependent on wave period, wave type (regular or irregular), and valve angle (damping).

1) *Wave Period*: Both regular and irregular wave conditions indicate a relationship of the interaction factor with the wave period. For our model's geometry and dimensions, the shorter periods are found to yield higher interaction factors and the longer periods lower interaction factors. However, all periods

TABLE III
INTERACTION FACTORS FROM
DIFFERENT WAVE SCENARIOS

Regular Waves			
Valve Angle	Period [s]	Interaction Factor	# of Generations
80°		2.8095	561
44°	1.22	2.5790	318
0°		2.5561	463
44°	1.57	1.4387	634
44°	1.91	1.1946	192
44°	2.26	1.1027	278
44°	2.61	1.0554	475
80°		1.0243	260
44°	3.31	1.0257	257
0°		1.0645	485
Irregular Waves			
Valve Angle	Peak Period [s]	Interaction Factor	# of Generations
80°		1.4559	306
44°	1.22	1.6745	316
0°		1.7597	483
44°	1.91	1.1406	445
44°	2.61	1.0646	520
80°		1.0465	208
44°	3.31	1.0392	500
0°		1.0723	453

we tested resulted in power production greater than what would be obtained by five devices acting in isolation. With a valve angle of 44° and regular waves, a period of 3.31 seconds results in an increase in power of 2.57% and a period of 1.22 seconds results in 158% power increase. Similarly the same valve angle but with irregular waves results in power increases of 3.69% and 67.5% respectively. The behavior of the device based on the power conveys the need to consider device design based on the sea states expected to be experienced.

2) *Wave Type (Regular and Irregular Behavior)*: Considering a 1.22 second wave period with corresponding valve angles of 80°, 44° and 0°, the regular wave scenarios perform much better than the irregular wave scenarios; however, for the same valve angles and a 3.31 second wave period, the regular wave scenarios perform slightly worse. This could be that for short-period, regular waves, the devices can position themselves to best take advantage of neighboring devices' diffracted waves due to the wave period consistency. As we noted previously, the arrays did not perform as well with longer periods and therefore the interaction factors are lower for both regular

and irregular waves. Consequently, the devices are not able to capitalize on each others' diffracted waves as well. Since some waves in an irregular wave climate will not have their energy efficiently captured by upwave devices, there is the possibility of developing a slightly enhanced wave condition behind the frontward devices. Comparatively, the wave consistency in regular wave conditions likely improves the energy capture efficiency. The overall best interaction factor of 181% occurs when the valve angle is 80° and regular waves with a short period are experienced. Conversely, the overall worst interaction factor of 2.43% is also found with a valve angle of 80° and in regular waves, but with a long wave period.

3) *Valve Angle (Damping)*: While the optimal layouts and corresponding interaction factors are dependent on the incident wave's period, there is also an observed dependency on the damping associated with the input valve angle (Table II). Keeping a fixed wave period we examine the interaction factors obtained by scenarios with valve angles of 80° , 40° and 0° . This is done for our evaluated wave period's upper and lower limits of 1.22 and 3.31 seconds. For the former period, the interaction factor increases with a decreased valve angle. For the period of 1.22 seconds, an interaction factor is found yielding a power increase of 45.4% when the valve angle 80° . This increases to 67.5% and 76.0% for valve angles of 44° and 0° respectively. When the period is 3.31 seconds, somewhat similar behavior is found with valve angles of 80° and 0° ; however, the value found for 44° is slightly less than that of the 0° . This is potentially due to a GA not guaranteeing global optimality. Upcoming studies will be conducted to further understand how damping might be correlated to optimal array configurations and interaction factor.

To evaluate the sensitivity of the power output when considering array optimization and active device control, we determined optimal layouts for irregular wave ($H_s = 0.136\text{m}$) at the wave periods ($T_p = 1.22\text{s}, 1.57, 1.91\text{s}, 2.26\text{s}, 2.61\text{s},$ and 3.31s) shown in Bosma et al. [1]. For each wave period, we consider the damping values associated with 10 different valve angles ranging from 0 to 80° .

Observing Fig. 10 we see that the largest improvement in interaction factor is primarily dependent on the experienced wave conditions and less on the valve angle. This reiterates the importance of including and considering both in array design. This figure also indicates the need to consider the sea state a device will experience when designing the device itself.

VII. CONCLUSION

To ensure that ocean wave energy is generating as much power as possible in order to be economically viable, two methods have been promoted as future means of bettering the power development of grid connected WEC arrays. These are the creation of automated schemes for array optimization and

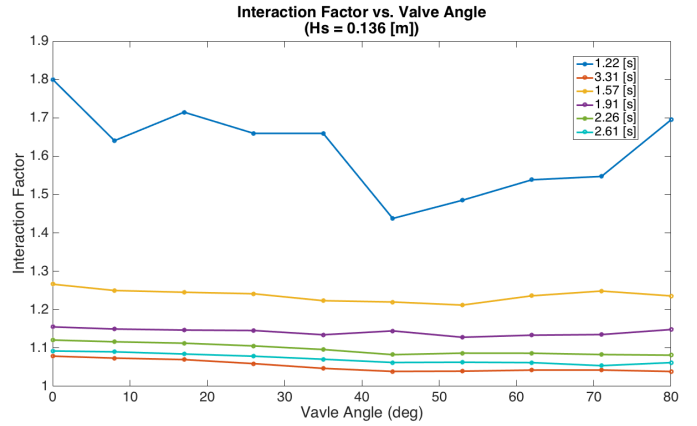


Fig. 10. INTERACTION FACTOR SENSITIVITY BASED ON VALVE ANGLE AND WAVE PERIOD

the development of advanced device controls.

To date, we have built a problem specific genetic algorithm for the generating of optimal arrays given power and preliminary cost. Previous results were of a generic device, but here we present the optimization of scaled oscillating water column arrays based on a validated BEM model of our device (see Fig. 3).

Optimal arrays are found for several different scenarios that differ based on wave type (regular and irregular), incident wave periods, and varied valve angles (damping). We observe that, while always greater than one, the interaction factor varies greatly depending on the incident wave periods. The lowest interaction factor when considering irregular waves shows a power improvement of 3.92% (valve angle of 80° and period of 3.31 seconds) while the largest shows improvement of 76.0% power increase (valve angle of 0° and period of 1.22 seconds).

The connection between the damping and the interaction factor is less clear, but does indicate the ability to obtain greater power based on the position of the valve. This information reveals the importance of concurrently implementing control in the future of array optimization, but also shows that the array design is equally if not more important. The interaction factor was influenced much stronger by the incident period than the damping.

So, while it is necessary to incorporate the two tools, we show that active control is not to be implemented without also considering device design given expected wave conditions. Variability of incident wave directions will potentially have a major effect on the power production of an array and could indicate an even greater need for combining array optimization and active device control. We are planning on incorporating this component as a next step.

This project has given us very useful results which will better our understanding regarding how to best approach the

conjoining of optimal array design and active device control as a fluid process.

ACKNOWLEDGMENT

This paper is based upon work supported by the United States Department of Energy under Award Number DE-EE0006816. Neither the United States Government nor any agency thereof, nor any of their employees, makes any warranty, expressed or (a) implied, or assumes any legal liability or responsibility for the accuracy, completeness, or usefulness of any information, apparatus, product, or process disclosed, or represents that its use would not infringe upon privately owned rights. Reference herein to any specific commercial product, process, or service by trade name, trademark, manufacturer, or otherwise does not necessarily constitute or imply its endorsement, recommendation, or favoring by the United States Government or any agency thereof. The views and opinions of the authors expressed herein do not necessarily state or reflect those of the United States Government or any agency thereof.

REFERENCES

- [1] B. Bosma, T. Brekken, P. Lomonaco, A. McKee, B. Paasch, and B. Batten, "Physical Model Testing and System Identification of a Cylindrical OWC Device," *12th European Wave and Tidal Energy Conference [accepted]*, 2017.
- [2] S. Bellew, T. Stallard, and P. K. Stansby, "Optimisation of a Heterogeneous Array of Heaving Bodies," in *8th European Wave and Tidal Energy*, 2009, pp. 1–9.
- [3] P. Balitsky, G. Bacelli, and J. V. Ringwood, "Control-influenced layout optimization of arrays of wave energy converters," in *ASME 2014 International Conference on Ocean, Offshore and Arctic Engineering*, 2014, pp. 1–10.
- [4] D. G. Wilson, G. Bacelli, R. G. Coe, D. L. Bull, O. Abdelkhalik, U. A. Korde, and R. D. Robinett, "A Comparison of WEC Control Strategies," Sandia National Laboratory, Tech. Rep., 2016.
- [5] C. M. Linton and D. V. Evans, "The Interaction of Waves with Arrays of Vertical Circular Cylinders," *Journal of Fluid Mechanics*, vol. 215, no. -1, p. 549, 1990.
- [6] S. a. Mavrakos and P. McIver, "Comparison of Methods for Computing Hydrodynamic Characteristics of Arrays of Wave Power Devices," *Applied Ocean Research*, vol. 1187, no. 97, pp. 283–291, 1998.
- [7] B. Borgarino, A. Babarit, and P. Ferrant, "Impact of wave interactions effects on energy absorption in large arrays of wave energy converters," *Ocean Engineering*, vol. 41, pp. 79–88, 2011. [Online]. Available: <http://dx.doi.org/10.1016/j.oceaneng.2011.12.025>
- [8] A. Babarit, "On the park effect in arrays of oscillating wave energy converters," *Renewable Energy*, vol. 58, pp. 68–78, 2013. [Online]. Available: <http://dx.doi.org/10.1016/j.renene.2013.03.008>
- [9] M. Vicente, M. Alves, and A. Sarmiento, "Layout optimization of wave energy point absorbers arrays," in *10th European Wave and Tidal Energy Conference*, 2013.
- [10] H. A. Wolgamot, P. H. Taylor, and R. E. Taylor, "The interaction factor and directionality in wave energy arrays," *Ocean Engineering*, vol. 47, pp. 65–73, 2012. [Online]. Available: <http://dx.doi.org/10.1016/j.oceaneng.2012.03.017>
- [11] P. M. Ruiz, F. Ferri, and J. P. Kofoed, "Sensitivity Analysis of WEC Array Layout Parameters Effect on the Power Performance," in *11th European Wave and Tidal Energy Conference*, no. 1, Nantes, France, 2015, pp. 1–8.
- [12] A. Nambiar, A. Collin, S. Karatzounis, J. Rea, B. Whitby, and A. Kiprakis, "Optimising Network Design Options for Marine Energy Converter Farms," in *11th European Wave and Tidal Energy Conference*, Nantes, France, 2015, pp. 1–10.
- [13] J. Cruz, R. Sykes, P. Siddorn, and R. E. Taylor, "Wave Farm Design : Preliminary Studies on the Influences of Wave Climate , Array Layout and Farm Control," in *8th European Wave and Tidal Energy Conference*, pp. 736–745.
- [14] W. Chen, F. Gao, X. Meng, and J. Fu, "Design of the wave energy converter array to achieve constructive effects," *Ocean Engineering*, vol. 124, pp. 13–20, 2016. [Online]. Available: <http://dx.doi.org/10.1016/j.oceaneng.2016.07.044>
- [15] J. C. McNatt, V. Venugopal, and D. Forehand, "A novel method for deriving the diffraction transfer matrix and its application to multi-body interactions in water waves," *Ocean Engineering*, vol. 94, pp. 173–185, 2014. [Online]. Available: <http://dx.doi.org/10.1016/j.oceaneng.2014.11.029>
- [16] C. Fitzgerald and G. Thomas, "A preliminary study on the optimal formation of an array of wave power devices." in *7th European Wave and Tidal Energy Conference*, 2007.
- [17] L. Mao, "Optimizing Wave Farm Layouts Under Uncertainty," Lehigh University, Tech. Rep., 2013.
- [18] L. V. Snyder and M. Moarefdoost, "Optimizing Wave Farm Layouts Under Uncertainty," Ph.D. dissertation, 2013.
- [19] M. M. Moarefdoost, L. V. Snyder, and B. Alnajjab, "Layouts for ocean wave energy farms: Models, properties, and optimization," *Omega (United Kingdom)*, vol. 66, pp. 185–194, 2017. [Online]. Available: <http://dx.doi.org/10.1016/j.omega.2016.06.004>
- [20] B. Child and V. Venugopal, "Optimal configurations of wave energy device arrays," *Ocean Engineering*, vol. 37, no. 16, pp. 1402–1417, nov 2010. [Online]. Available: <http://linkinghub.elsevier.com/retrieve/pii/S0029801810001447>
- [21] D. Sarkar, E. Contal, N. Vayatis, and F. Dias, "Prediction and Optimization of Wave Energy Converter Arrays Using a Machine Learning Approach," *Renewable Energy*, vol. 97, pp. 504–517, 2016. [Online]. Available: <http://linkinghub.elsevier.com/retrieve/pii/S0960148116304931>
- [22] J. Wu, S. Shekh, N. Y. Sergiienko, B. S. Cazzolato, B. Ding, F. Neumann, and M. Wagner, "Fast and Effective Optimisation of Arrays of Submerged Wave Energy Converters," in *Genetic and Evolutionary Computation Conference*, 2016, pp. 1–8.
- [23] J. P. L. McGuinness and G. Thomas, "Optimal Arrangements of Elementary Arrays of Wave-Power Devices," in *11th European Wave and Tidal Energy Conference*, Nantes, France, 2015, pp. 1–10.
- [24] C. Sharp and B. DuPont, "Wave Energy Converter Array Optimization A Review of Current Work and Preliminary Results of a Genetic Algorithm Approach Introducing Cost Factors," in *ASME 2015 International Design Engineering Technical Conference & Computers and Information in Engineering Conference*. ASME, 2015, pp. 1–10.
- [25] —, "A Multi-Objective, Real-Coded Genetic Algorithm Method for Wave Energy Converter Array Optimization," in *ASME 2016 35th International Conference on Ocean, Offshore and Arctic Engineering*, 2016, pp. 1–10.
- [26] WAMIT Inc., "WAMIT V7.2 User Manual." WAMIT Inc., 2016.
- [27] D. Evans, "The Oscillating Water Column Wave Energy Device," *IMA Journal of Applied Mathematics*, vol. 22, no. 4, pp. 423–433, 1978.
- [28] M. Penalba and J. V. Ringwood, "A review of wave-to-wire models for wave energy converters," *Energies*, vol. 9, no. 7, 2016.
- [29] I. Simonetti, L. Cappiotti, H. El Safti, and H. Oumeraci, "Numerical Modelling of Fixed Oscillating Water Column Wave Energy Conversion Devices: Toward Geometry Hydraulic Optimization," *Volume 9: Ocean Renewable Energy*, vol. 9, p. V009T09A031, 2015. [Online]. Available: <http://www.scopus.com/inward/record.url?eid=2-s2.0-84947724837}&partnerID=tZOTx3y1>
- [30] W. Sheng, A. Lewis, and R. Alcorn, "Numerical Studies on Hydrodynamics of a Floating Oscillating Water Column," pp. 1–8, 2011.
- [31] T. Kelly, T. Dooley, J. Campbell, and J. Ringwood, "Modelling and Results for an Array of 32 Oscillating Water Columns." *EWTEC 2013 Proceedings*, 2013. [Online]. Available: http://www.eeng.nuim.ie/coer/doc/PUB0050{_}615-ThomasKelly.pdf
- [32] J. C. McNatt, V. Venugopal, and D. Forehand, "The cylindrical wave field of wave energy converters," *International Journal of Marine Energy*, vol. 3-4McNatt, pp. e26–e39, dec 2013. [Online]. Available: <http://linkinghub.elsevier.com/retrieve/pii/S2214166913000350>